

# Effect of surface pinning on magnetic nanostructures

Aditi Sahoo,<sup>1</sup> Dipten Bhattacharya,<sup>1</sup> and P. K. Mohanty<sup>2</sup>

<sup>1</sup>*Advanced Mechanical and Material Characterization Division,  
CSIR-Central Glass and Ceramic Research Institute,  
196, Raja S.C Mullick Road, Kolkata, 700032 India*

<sup>2</sup>*CMP Division, Saha Institute of Nuclear Physics,  
HBNI, 1/AF Bidhan Nagar, Kolkata, 700064 India*

(Dated: November 16, 2021)

Magnetic nanostructures are often considered as highly functional materials because they exhibit unusual magnetic properties under different external conditions. We study the effect of surface pinning on the core-shell magnetic nanostructures of different shapes and sizes considering the spin-interaction to be Ising-like. We explore the hysteresis properties and find that the exchange bias, even under zero field cooled conditions, increases with increase of, the pinning density and the fraction of up-spins among the pinned ones. We explain these behavior analytically by introducing a simple model of the surface. The asymmetry in hysteresis is found to be more prominent in a inverse core-shell structure, where spin interaction in the core is antiferromagnetic and that in the shell is ferromagnetic. These studied of inverse core-shell structure are extended to different shapes, sizes, and different spin interactions, namely Ising, XY- and Heisenberg models in three dimension. We also briefly discuss the pinning effects on magnetic heterostructures.

## I. INTRODUCTION

In recent few years, nanomaterial has become one of the interesting field of research [1, 2] as it shows important novel properties in mesoscopic scale [3]. The nanoparticles have been in the center of attention of researchers for many years as the change of scale from micro- to nanometer increases the surface to volume ratio leading to a drastic change in the chemical and physical properties of the system [4]. Nano-particles can be synthesized with different spatial structures, like nano-composites, heterostructure and core-shell structure, etc. [2, 5, 6].

Heterostructures are layered composites prepared from combination of materials [7, 8] having different physical properties like ferromagnetic-antiferromagnetic, superconductor-ferromagnetic, semiconductor-ferromagnetic, etc.. These combination produces a rich variety of novel physical phenomena strikingly different from the individual constituents. The examples include large exchange bias [9, 10], giant magneto-resistance [11], varied interlayer exchange coupling [12], unusual spin transport [13].

Another interesting structure is a core-shell structure which is found naturally [14], or can be produced as a nano-particles in the lab [15, 16]. Study of core-shell nanostructures have become popular recently as they find strong potential applications in different fields of research like biomedical [17, 18], catalysts [19], memory device application [20] etc., as their magnetic properties can be varied easily by changing the size, shape, core or shell thickness, or other intrinsic properties. These materials can be used for magnetic switching [21], magnetotransport [22], micromechanical sensors [23], DNA separation [24], magnetic memory device[25]. bio-imaging and mag-

netic resonance imaging enhancement [26], targeted drug delivery [27], etc..

The core-shell structure can be of different types : (i) magnetic core-non magnetic shell [28], (ii)magnetic core-ferri or anti-ferromagnetic shell [29], (iii) magnetic core-plasmonic shell [30], (iv) polymar core-semiconductor shell [31], (v) metallic core-metallic shell [32]. The unusual magnetic properties observed in all these different structures owes to their mesoscopic scale, where size and shape-anisotropy play an important role. It is known that the change in preferential orientation of magnetic easy-axis is responsible for changing the value of coercivity [33]. The microscopic origin of the exchange bias however depends on many details, like the thickness of core and shell [34], anisotropic spin interaction[35] and interaction in the core-shell interface [36]. In addition, pinning of spins at the interface [37] or at the the surface [38] can affect the magnetic behavior strongly.

In this article we study how spin pinning on the surface affects the hysteresis properties of the magnetic core-shell structure. First we consider a circular core-shell structure where Ising spins on lattice sites belonging to the core interact antiferromagnetically whereas those in the shell interact ferromagnetically. The interaction in the interface can be ferro or antiferromagnetic in nature. Spins on the surface, which are part of the shell, also interact ferromagnetically but some of the these spins are pinned in a sense that their orientation does not change with time. Monte Carlo simulations of the core-shell structure reveals that the exchange bias strongly depends on the fraction of  $\uparrow$ -spins among the pinned ones, and the pinning density. A simple model of the surface is introduced to understand these properties. We also investigate the magnetic properties of core-shell structure of different shapes: elliptical, square, triangular and some irregular

shapes and verify that surface pinning indeed affect the coercivity and exchange bias strongly. For continuous spin variables, in XY- or Heisenberg models, the magnetic transitions can occur only in three dimension. We compare the magnetic properties of core-shell nanostructure in three dimension, with different spin interactions following Ising, XY and Heisenberg models. These studies are also extend to magnetic heterostructures, where spins in the bottom layers interact antiferromagnetically whereas interaction in the top layers is ferromagnetic. Interestingly, we find that the coercive field in the reverse direction of the hysteresis loop can become positive when the number of ferromagnetic layers are decreased below a threshold value.

## II. THE MODEL

We intend to study, primarily, the magnetic properties of core-shell nanostructures. We assume that the external temperature is smaller than the critical threshold  $T_c$  above which the magnetic order disappears. Simple models which undergo magnetic transition at some finite temperature  $T_c \neq 0$ , are Ising model in two and three spatial dimensions ( $d = 2, 3$ ), XY model in three dimension ( $d = 3$ ) and Heisenberg model in three dimension ( $d = 3$ ). This is because the non-existence theorem [39] rules out possibility of finite temperature phase transition in one dimension (1d) and the Mermin-Wagner [40] theorem does not allow continuous symmetry, one like the planar spins in XY model or three dimensional spins with unit magnitude in Heisenberg model, to be broken in  $d \leq 2$ .

Let us consider a disk-like nanoparticles in  $d = 2$  with constituent spins having Ising symmetry. This is the simplest model that exhibits intrigue and interesting magnetic properties in mesoscopic scale when the surface spins are pinned. A generalization to spherical particles in three dimension with spins following Ising, XY or Heisenberg symmetry is straight forward; we discuss these cases briefly in section VI.

We consider a square lattice with circular boundaries of radius  $R$ , which has a circular core  $\mathcal{C}$  of radius  $R_c < R$ ; the shell region  $\mathcal{S}$  falls between these two circles (see Fig. 1). Each lattice site  $i$  of this core-shell structure is associated with a Ising spin  $s_i = \pm 1$  (representing  $\uparrow, \downarrow$ ) which interact following the Hamiltonian,

$$\begin{aligned} \mathcal{H} = & -J_c \sum_{i \in \mathcal{C}, j \in \mathcal{C}} s_i s_j - J_{sh} \sum_{i \in \mathcal{S}, j \in \mathcal{S}} s_i s_j \\ & - J_{int} \sum_{i \in \mathcal{S}, j \in \mathcal{C}} s_i s_j - H \sum_{i \in \mathcal{C}, i \in \mathcal{S}} s_i, \end{aligned} \quad (1)$$

where  $j$  is the nearest neighbor of site  $i$ ,  $J_c$  ( $J_{sh}$ ) are the exchange interaction among the spins within the core (shell),  $J_{int}$  represents core-shell interface interaction and

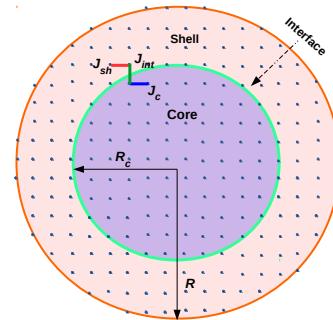


FIG. 1: (Color online) Schematic representation of the core-shell structure: The core-shell structure in two dimension is represented here by a square lattice bounded by a circle of radius  $R$ , within which there is a circular-core having radius  $R_c < R$ ; the annular region of width  $R - R_c$  is the shell. Ising spins  $s_i = \pm 1$ , on the lattice sites belonging to the core (shell) interact with strengths  $J_c$  ( $J_{sh}$ ) and the interaction strength across the interface is  $J_{int}$ .

$H$  is the external magnetic field. Obviously, the spins interact ferromagnetically (antiferromagnetically) when the corresponding value of interaction strength is positive (negative); for example when  $J_c < 0$ , and sites  $i$  and  $j$  are within the core ( $i \in \mathcal{C}$  and  $j \in \mathcal{C}$ ) the spins  $s_i$  and  $s_j$  interact antiferromagnetically. The magnetic field  $H$  is experienced by all the spins, both in core  $\mathcal{C}$  and shell  $\mathcal{S}$ . In addition, to mimic surface pinning which has been observed in magnetic nanoparticles in contact of organic liquids [41], in ferromagnetic thin films [42] and core-shell structures [38] etc., we assume that  $\eta$ -fraction of boundary spins are pinned; a parameter  $0 \leq r \leq 1$  controls the fractions of  $\uparrow$  spins among pinned ones.

We proceed by assuming the interaction of spins within the core is antiferromagnetic ( $J_c < 0$ ) whereas the interaction of spins in the shell is ferromagnetic ( $J_{sh} > 0$ ) and the interaction at the interface can be ferro- or antiferromagnetic; this is not the usual scenario but observed in several experimental systems [43]. We briefly discuss other possible structures in section III B. In the following we primarily study the hysteresis effects, particularly the dependence of coercive field and exchange bias change on different model parameters and the shape and size of the core-shell structure.

## III. CORE-SHELL STRUCTURES IN TWO DIMENSION

### A. Anti-ferromagnetic core and Ferromagnetic shell

We start with nanoparticles having a circular core-shell structure with radius  $R_c$  and  $R$  respectively. The inter-

action among spins is described by the Hamiltonian Eq. (1), with three exchange coupling constants  $J_c, J_{sh}, J_{int}$  and the external field  $H$ . We proceed to do the Monte Carlo (MC) simulations of the model at temperature  $\beta^{-1} = 1$  and pinning density  $\eta$ . Thus, the total number of pinned spins is  $N = \eta L$  where  $L$  is number of lattice sites on the surface - these  $N$  spins are chosen out of  $L$  randomly and independently. Further, we choose  $rN$  spins out of  $N$  randomly and orient them  $\uparrow$ ; the rest of them points  $\downarrow$ .

We start the simulation from a random configuration where all spins in the core and the shell, except those which are pinned, are chosen to be  $\uparrow$  (+) or  $\downarrow$  (-) with equal probability, that mimics an Ising configuration at infinite temperature and zero magnetic field. In this zero-field condition, we set the temperature of the system  $\beta^{-1} = 1$  and keep it fixed throughout the simulation [44]. To obtain hysteresis we first raise the magnetic field slowly from  $H = 0$  to  $H_{max} = 2$  with a rate 0.02 units per Monte Carlo sweep (MCS) and finally the hysteresis loop calculations are undertaken for a cycle, by varying the field from  $H_{max}$  to  $-H_{max}$  and then to  $H_{max}$  again with same rate. Magnetization of the system is measured after each MCS and it is averaged over 100 samples. We primarily focus on the dependence of coercive field ( $H_c$ ) and exchange bias field ( $H_{eb}$ ) on pinning density  $\eta$ ,  $\uparrow$ -spin fraction  $r$ , interface interaction strength  $J_{int}$  and core-shell size  $R_c, R$ .

The coercivity  $H_c$  and exchange bias  $H_{eb}$  in a hysteresis loop are defined as

$$H_c = \frac{1}{2}(H_{c2} - H_{c1}) \quad \text{and} \quad H_{eb} = \frac{1}{2}(H_{c2} + H_{c1}), \quad (2)$$

where  $H_{c2}$  and  $H_{c1}$  are the fields corresponding to zero magnetic moment in the forward and reverse branches of the loop (as shown in Fig. 2(a)). Usually the coercive field  $H_{c1}$  is negative and  $H_{c2}$  is positive. The exchange bias, however, can change sign; it is positive (negative) when  $|H_{c1}| < |H_{c2}|$  ( $|H_{c1}| > |H_{c2}|$ ). In ordinary of asymmetry in the hysteresis. In the following we see that, surface pinning can produce non-zero exchange bias in core-shell magnetic nanoparticles.

Now, we study how hysteresis properties change when one of the model parameters changes, while the others are taken from the following default values, unless otherwise specified.

$$\begin{aligned} R &= 32, R_c = 26, \eta = 0.4, r = 0.7, \\ J_c &= -0.5, J_{sh} = 1, J_{int} = 1. \end{aligned} \quad (3)$$

*Dependence of  $H_{eb}, H_c$  on  $\eta$* : First we study the hysteresis properties of a nanoparticle by changing the pinning density  $\eta$ . Other parameters are kept fixed at the default values given in Eq. (3). In Fig. 2(a) we present hysteresis loops for different  $\eta$ . These loops show negative exchange bias which increases as the pinning density

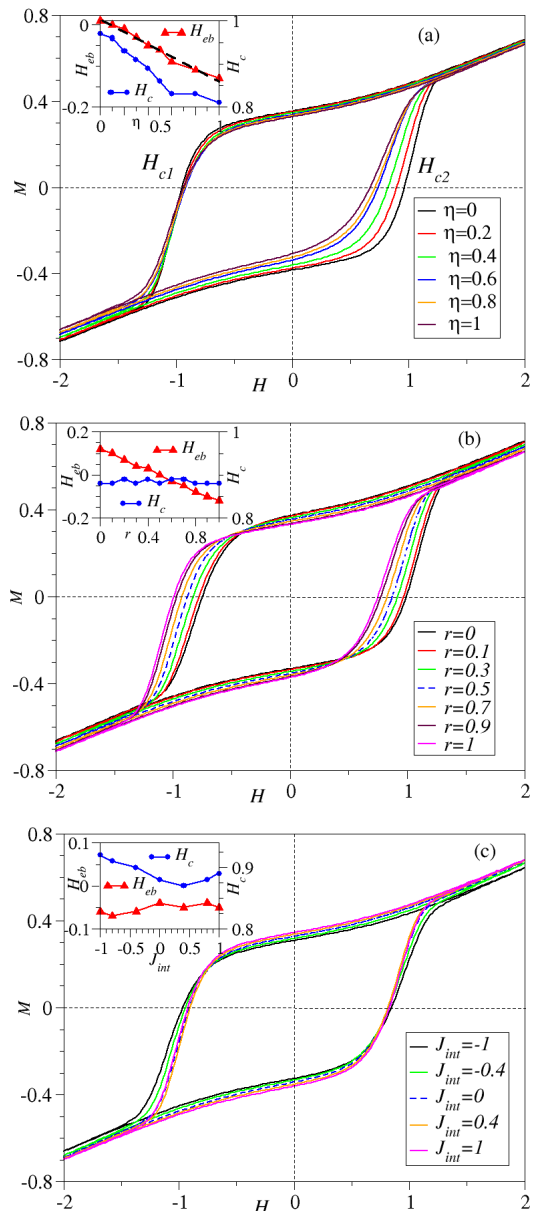


FIG. 2: (Color online) The main figures show hysteresis loops for two-dimensional circular core-shell structure when one of the model parameters  $X$  is changed while other parameters are taken from Eq. (3); insets show the corresponding change in coercivity  $H_c$  and exchange bias  $H_{eb}$ . (a)  $X = \eta$ :  $H_c$  decreases, but  $|H_{eb}|$  increases with increase of  $\eta$ . The dashed line is the best linear fit  $H_{eb} = -0.15\eta + 0.013$ . (b)  $X = r$ :  $H_c$  is almost a constant, but  $|H_{eb}|$  increases linearly with increase of  $\eta$ . (c)  $X = J_{int}$ : No appreciable change in  $H_c$  and  $|H_{eb}|$ .

$\eta$  is increased. The exchange bias is maximum when all the spins are pinned to the surface. The reason of the asymmetry in the loop is that 70% of the pinned spins are  $\uparrow$  and thus one requires some additional magnetic field to completely reverse the magnetization. The coercivity, however, decreases with increase of  $\eta$ . This is

because, with increase of pinning density more spins of ferromagnetic shell are pinned and less number spins of the shell take part in the ferromagnetic dynamics - which effectively decrease the shell width.

*Dependence of  $H_{eb}$ ,  $H_c$  on  $r$*  : Different external conditions pins the spins on the surface differently. If the cause of pinning is organic solvent, both the density of pinned spins and the  $\uparrow$ -spin fraction may vary in different solvent conditions. Here we intend to change  $\uparrow$ -spin fraction  $r$  and investigate the hysteresis properties. For  $r > \frac{1}{2}$ , more  $\uparrow$ -spins are pinned compared to the  $\downarrow$  and one expects that an effective positive intrinsic field is generated in the system. Thus, one needs some additional negative external magnetic field to nullify this effect, resulting in a negative exchange bias. Similarly, a positive exchange bias is expected for  $r < \frac{1}{2}$ . In Fig. 2(b) we have plotted the hysteresis curves for different  $r$ , keeping  $\eta = 0.4$  and other parameters same as that in Eq. (3). The inset here shows dependence of  $H_{eb}$  and  $H_c$  on  $r$ . As expected,  $H_{eb} = 0$  for  $r = \frac{1}{2}$ , it is negative (positive) for  $r > \frac{1}{2}$  ( $r < \frac{1}{2}$ ), and  $|H_{eb}|$  increases as one moves away from  $r = \frac{1}{2}$ . The coercivity, which primarily depends on the pinning density  $\eta$ , is almost independent of  $r$ .

*Dependence of  $H_{eb}$ ,  $H_c$  on  $J_{int}$*  : Now we aim at changing  $J_{int}$ , the interface interaction strength. The hysteresis loops for a particles with size  $R = 32$  and  $R_c = 26$  are plotted in Fig. 2(c) With change of  $J_{int}$  we do not find any significant change in  $H_c$  and  $H_{eb}$ ; two extreme values  $J_{int} = 1, -1$  gives rise to a slightly increased coercive field, but the exchange bias changes only a little. Thus, it appears that in a core-shell magnetic system the exchange bias can be controlled effectively by the  $\uparrow$ -spin pinning fraction  $r$  and the pinning density  $\eta$ , not by the interface interaction  $J_{int}$ .

One should note that some earlier studies have reported a significant change in exchange bias with change in interface interaction strength  $J_{int}$  [36]. These studies, primarily focus on core-shell structure with ferromagnetic core and antiferromagnetic shell [45–47], modeled by the usual Heisenberg model in three dimension along with, additional magnetic anisotropy [45, 46] and sometimes in presence of a crystal field [48]. In addition hysteresis is studied in both field cooled and zero-field cooled conditions; the exchange bias and its change with respect to interface interactions are found to be significant only in field cooled conditions [36].

In the present study we have an inverse core-shell structure, with an antiferromagnetic core and ferromagnetic shell modeled by Ising spins in two dimension and there is no magnetic anisotropy or any crystal field; in this simple case, even in zero-field cooled conditions we find a large exchange bias  $H_{eb}$  when surface spins are pinned.  $H_{eb}$  will, of course, increase further in field cooled conditions. To emphasize that surface-pinning indeed causes large exchange bias, we extend the study to three dimensional inverse core-shell structure considering Ising, XY-

and Heisenberg models (see section VI); in all these cases, under zero field cooled conditions, the affect of  $J_{int}$  on  $H_{eb}$  are found to be negligible.

*Dependence of  $H_{eb}$ ,  $H_c$  on  $R$  and  $R_c$*  : Figure 3(a) shows the hysteresis loops of inverted core-shell structure for different  $R_c$ , keeping  $R = 32$  fixed; thus the shell thickness increases with decrease of  $R_c$ . The other parameters are chosen from Eq. (3). In Fig. 3(a) we plot the variation of coercive field and exchange bias with  $R_c$ . Here,  $|H_{eb}|$  increases with increase of  $R_c$  and reaches a constant value asymptotically. The saturation magnetization and coercive field, however, decreases for larger  $R_c$ . This is because, the coercivity primarily gets contribution from the ferromagnetic shell (antiferromagnetic core produces zero net magnetic moment) whose thickness decreases with increased  $R_c$ .

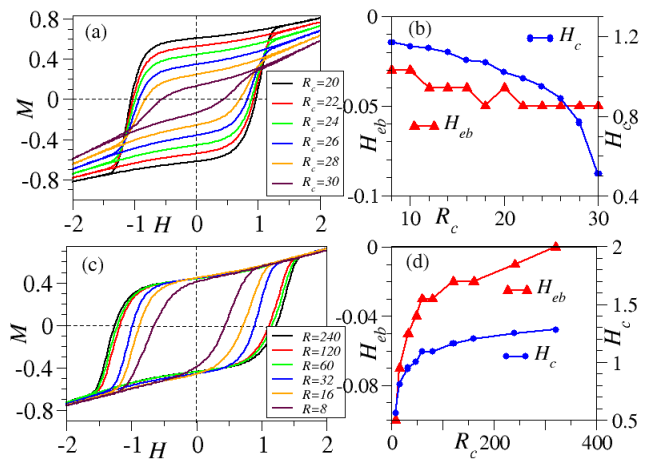


FIG. 3: (Color online) (a) Hysteresis loops for different shell thickness  $R - R_c$ , obtained by varying  $R_c$ , keeping  $R = 32$  fixed. (b)  $|H_{eb}|$  increases with increase  $R_c$  and reach a constant for large  $R_c$ .  $H_c$  also decreases with increase of  $R_c$ , as the number of ferromagnetic layers also decrease. (c) The thermodynamic limit of the system can be achieved by changing the size of the core and shell proportionately. Here we plot hysteresis loops for different  $R$ , and fixed  $\frac{R_c}{R} = \frac{3}{4}$ . (d)  $H_c, H_{eb}$  as a function of  $R$ .  $H_c$  increases with  $R$  as the number of ferromagnetic layers increase. However  $H_{eb} \rightarrow 0$  because the surface (where pinning occurs) to volume ratio approaches to zero in the thermodynamic limit. Unspecified parameters here are taken from Eq. (3).

It is important to ask whether the observed behavior is scalable, i.e., whether the asymmetric hysteresis survives in the thermodynamic limit where  $R_c$  and  $R$  increases keeping their ratio fixed. To study this we increase particle size  $R$  while increasing the core size  $R_c$  proportionately,  $R_c = \frac{3}{4}R$ . Other parameters are taken as those in Fig. 3(a). We find, in Fig. 3(c) that the size of hysteresis loop increase with  $R$ , as the number of ferromagnetic layers are increased. This is reflected in increased value of coercivity in Fig. 3(d). However,

the magnitude of the exchange bias  $|H_{eb}|$  decreases with  $R$  indicating the asymmetry of the loop decreases with  $R$  and one gets a usual symmetric hysteresis in thermodynamic limit. Thus, the exchange bias due to surface pinning are only the mesoscopic effects which goes away in larger systems when surface to volume ratio becomes very small. In fact, similar size dependence of coercivity and  $H_{eb}$  has been observed in system with ferromagnetic shell and antiferromagnetic core [34, 49].

## B. Ferromagnetic core or Antiferromagnetic Shell

The core-shell structure that we studied so far has ferromagnetic interaction in the shell and antiferromagnetic interaction in the core. We have investigated the other possibilities too. The affects of surface pinning turned out to be not that prominent when the core (shell) is ferromagnetic (antiferromagnetic) irrespective of the interaction in the shell (core). We decide not to present these studies in details as these results neither add any significant information nor alter the conclusions of this article.

When spins interact ferromagnetically in the shell, the pinning of surface spins (which belong to the shell) can produce an effective additional magnetic field which in turn generate an asymmetry in the hysteresis loop. On the other hand, when spin interactions in the shell is antiferromagnetic, the pinning is less effective as other spins in the shell can orient in a direction opposite to the pinned spins and make an antiferromagnetically ordered structure throughout; thus, the effective intrinsic field produced in the system is negligible. In this case some sites might encounter frustrations and may give rise to certain local residual magnetic moment, but the number of the frustrated spins are statistically very small. On the other hand, when the core is ferromagnetic, one generally gets a large hysteresis loops even in absence of surface pinning because the volume of the core is usually much larger compared to that of the shell. Thus, the relative change of exchange bias and coercivity produced by surface pinning is quite small.

In summary, surface pinning surely affects the hysteresis properties in core-shell nanostructures but the effect is more prominent when interaction in the core is antiferromagnetic and that in the shell is ferromagnetic.

## C. Different surface morphology

Like other nanomaterials [50], the surface morphology or shape of a core-shell nanocomposites may be changed. Morphology of the nanoparticle can be spherical [51], square [49], elliptical [52], triangular [53] or it may be irregular [54]. Their magnetic properties depend crucially on the surface anisotropy [55]. Other properties like cat-

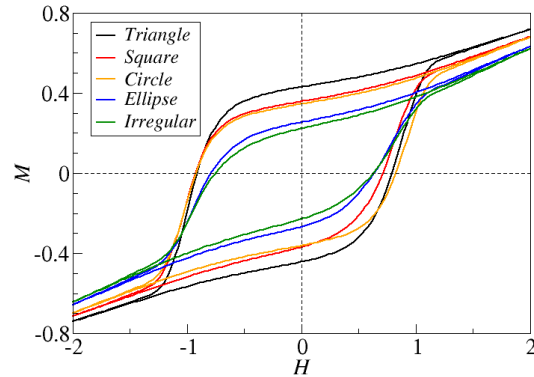


FIG. 4: (Color online) Shape dependence of magnetic hysteresis of core-shell nanoparticles for (i) equilateral triangle (base  $a = 86$ ), (ii) square ( $a = 56$ ), (iii) circle ( $R = 32$ ), (iv) ellipse (major and minor axis  $a = 46$ ,  $b = 23$ ) and (v) an irregular shape (core radius  $R_c = 26$ ). Each one has approximately same particle size and the shell thickness. Corresponding  $H_c = 0.86, 0.83, 0.89, 0.72, 0.7$  and  $H_{eb} = -0.06, -0.11, -0.05, -0.08, -0.06$ . Unspecified parameters are taken as the default values given in Eq. (3).

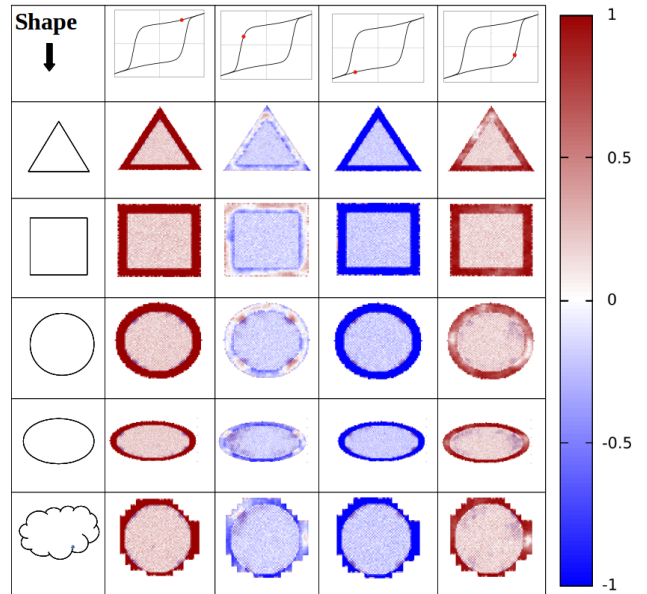


FIG. 5: (Color online) The spin configuration of inverse core-shell structure of different shapes, measured at four different positions in hysteresis loop, as indicated by  $\bullet$ . Particle size and other parameters are same as in Fig. 4.

alytic activity, electrical and optical properties are also highly shape dependent [56]. Combination of core-shell materials in different dimensions and shapes are designed

regularly for their potential application in technology, like magneto-plasmonic application [30], fluorescence application [57]. In this section we have studied hysteresis properties of two dimensional core-shell nanostructures having different shapes.

To emphasize how *change in surface morphology* affects the magnetic properties, we did Monte Carlo simulation of core-shell nanoparticles of different shapes, but similar area and shell-thickness. Coercivity and exchange bias obtained for different shapes are compared with that of the circular core-shell structure with  $R = 32$  and  $R_c = 26$ .

We consider four different shapes, (i) a triangular core-shell structure with base  $a = 86$ , (ii) a square core-shell structure with side  $a = 56$ , (iii) an elliptical core-shell structure with major axis  $a = 46$  and minor axis  $b = 23$  and (iv) a core-shell structure with irregular surface but circular core or radius  $R_c = 26$ . In all cases except (iv), the shell thickness is taken to be 6 lattice units and for (iv) the average thickness is  $\simeq 6$ . The interaction parameters  $J_c = -0.5$ ,  $J_{sh} = 1$ ,  $J_{int} = 1$  and the pinning parameters  $\eta = 0.4$ ,  $r = 0.7$  are kept same. Hysteresis loops of all these different shapes, along with that of the circle, are plotted in Fig. 4. Coercive field of circular shape is found to be maximum; then they are decreasing in order: circle, triangle, square, ellipse, and the irregular shape. The corresponding exchange biases are  $H_{eb} = -0.05, -0.06, -0.11, -0.08$  and  $-0.06$  respectively.

*Local magnetic structure* : The local magnetic structure changes during the hysteresis cycle. It is interesting to ask, how does the pinned spins on surface of a core-shell nanoparticle with different morphology, affects the local magnetic structure. To produce the hysteresis loop we take  $H_{max} = 2$  and now look at the spin configuration at four different positions in the hysteresis cycle, i.e., both in the forward and backward directions, at  $H = \pm 1$ . The configurations are averaged over 100 statistical samples to get the local magnetization profile  $\{m_i\} = \{\langle s_i \rangle\}$ . A density plot of the magnetization profile is shown in Fig. 5.

*Aspect ratio*: We notice that the coercivity of the elliptical core-shell structure is smaller than that of the circular one with same area. This indicates that rod-like structure may have the smallest coercivity, which indeed has been observed earlier [58]. Here we aim at studying systematically, how aspect ratio affects  $H_{eb}$  and  $H_c$ . To this end, we change the aspect ratio  $\alpha = \frac{a}{b}$  of the ellipse and follow the change in its magnetic properties. Figure 6 shows the hysteresis loops; the coercivity and exchange bias are plotted in the inset as a function of the aspect ratio. The interaction parameters and the pinning parameters are taken same as earlier. Note, that the coercive field  $H_c$  decreases, but  $|H_{eb}|$  increases as the aspect ratio  $\alpha$  increases.

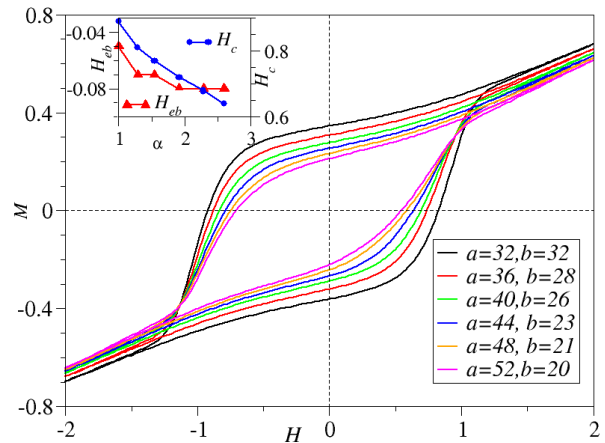


FIG. 6: (Color online) Hysteresis loop of elliptical core-shell structures, with approximately same area but different aspect ratio  $\alpha = a/b$ . All other parameters are taken from Eq. (3). The inset shows that the coercivity  $H_c$  decreases, but  $|H_{eb}|$  increases with  $\alpha$ .

#### IV. HETEROSTRUCTURES

The effects of surface pinning are also expected to be felt in heterostructures at nano-scale. Heterostructures are layered magnetic composites; we model them as  $N_F$  number of ferromagnetic layers placed on the top of  $N_{AF}$  number of antiferromagnetic layers. We have seen that in core-shell structure, where core to shell ratio is usually high, the surface-pinning affects the system strongly when the core is antiferromagnetic and shell is ferromagnetic; in other words affect of pinning is stronger when anti-ferro to ferro ratio is large. Should we expect the same here, i.e. whether the surface pinning would affect the magnetic properties of heterostructures strongly when  $N_{AF} > N_F$ ?

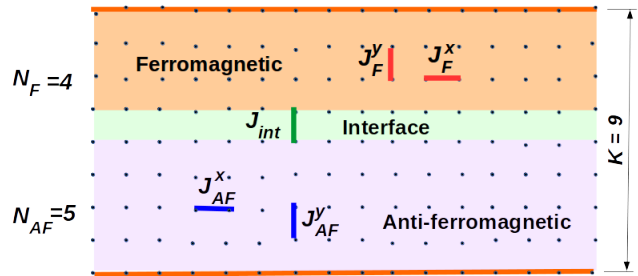


FIG. 7: (Color online) Schematic representation of the heterostructure of  $K$  layers (each containing  $L$  sites) of which  $N_{AF} = 5$  layer are antiferromagnetic and  $N_F = 4$  ferromagnetic. The intra-layer coupling strengths in ferro and antiferro layers are respectively  $J_{F,AF}^x$  and interlayer coupling strengths are  $J_{F,AF}^y$ . The interaction at the interface is  $J_{int}$ .

In two dimension, the layers can be modeled by a line

segment of length  $L$ , lattice sites  $i = 1, 2, \dots, L$ . The heterostructure is a composite of  $N_F$  antiferromagnetic layers placed one on the top of  $N_{AF}$  antiferromagnetic layers. The spins of the heterostructure are denoted by  $s_i^k = \pm 1$ , with  $i = 1, 2, \dots, L$ , and a layer index  $k = 1, 2, \dots, K = N_{AF} + N_F$  (see Fig. 7). The intralayer interaction strength of Ising spins in ferromagnetic (antiferromagnetic) layers are  $J_F^x$  ( $J_{AF}^x$ ), whereas the same in interlayer are  $J_F^y$  ( $J_{AF}^y$ ). At the interface the interaction strength is  $J_{int}$  which may be positive (ferro) or negative (antiferro). Corresponding Hamiltonian is,

$$\begin{aligned} \mathcal{H} = & -J_{AF}^x \sum_{k=1}^{N_{AF}} \sum_{i=1}^{L-1} s_i^k s_{i+1}^k - J_F^x \sum_{k=N_{AF}+1}^{N_F} \sum_{i=1}^{L-1} s_i^k s_{i+1}^k \\ & -J_{AF}^y \sum_{k=1}^{N_{AF}-1} \sum_{i=1}^{L-1} s_i^k s_i^{k+1} - J_F^y \sum_{k=N_{AF}+1}^{N_F-1} \sum_{i=1}^{L-1} s_i^k s_i^{k+1} \\ & -J_{int} \sum_{i=1}^{L-1} s_i^{N_{AF}} s_i^{N_{AF}+1} - H \sum_{k=1}^K \sum_{i=1}^L s_i^k \end{aligned} \quad (4)$$

We also consider pinning of spins, which occurs at the top layer  $k = K$  and the bottom layer  $k = 1$ . In the simulations, starting from a random initial condition and fixed temperature  $\beta^{-1} = 1$ , we first increase the field from  $H = 0$  to  $H = H_{max} = 2$  with a rate 0.02 units per MCS. The zero field hysteresis cycle is constructed now by varying the field from  $H = 2$  to  $H = -2$ , and then back to  $H = 2$ .

First we calculate the variation of coercivity  $H_c$  and exchange bias  $H_{eb}$  by varying the number of ferromagnetic layers  $N_F$  for a fixed number of antiferromagnetic layers  $N_{AF} = 24$ , as shown in Fig. 8 (a). The interaction parameters are taken to be  $J_{AF}^x = J_{AF}^y = J_{AF} = -0.5$ ,  $J_F^x = J_F^y = J_F = 1$ . At the interface, we have  $J_{int} = 1$ . The pinning parameters are, the pinning density  $\eta = 0.4$  and the  $\uparrow$ -spin fraction  $r = 0.7$ . Corresponding  $H_{c1}$  and  $H_{c2}$  are shown in Fig. 8 (b) in dashed line; the solid lines there correspond to  $N_{AF} = 8, 16$ . In these systems we find that the coercivity of the heterostructure decreases monotonically as  $N_F$  decreases.

We also find an interesting finite size effect which is worth of mention. In the usual hysteresis cycle the coercive field  $H_{c1}$  is negative. However, in heterostructure studied here, it appears that the  $H_{c1}$  can become positive when there are three or less ferromagnetic layers irrespective of antiferro-layers  $N_{AF}$  present. It is clear from Fig. 8 (b) that, for all three values of  $N_{AF} = 8, 16, 24$ , the coercive field  $H_{c1}$  becomes positive when  $N_F \leq 3$ .

Does this finite size effect originate from surface pinning? To answer this, we further study the hysteresis loop for different  $r$ , the  $\uparrow$ -spin fraction. Figure 8 (c) shows hysteresis curves for a heterostructure of  $N_{AF} = 8$  and  $N_F = 3$  layers, for different  $r = 0.55, 0.75, 1..$  In all cases,  $H_{c1}$  is positive ( $H_{c2}$  is also positive naturally). For this heterostructure, variation of  $H_{c1}$  as a function of  $r$

is shown (dashed line) in Fig. 8 (d), which clearly shows that  $H_{c1}$  crosses over from a negative value to a positive one at some threshold  $r = r^* \simeq 0.6$ . In the same figure, we also plot  $H_{c1}$  versus  $r$  for different heterostructures with three ferromagnetic layers, and different number of antiferro-layers  $N_{AF} = 16, 24$ ; here too  $r^* \simeq 0.6$ . In fact, the value of  $r^*$  depends strongly on the number of ferromagnetic layers  $N_F$  and its dependence of antiferromagnetic layers  $N_{AF}$  is negligibly small. We find,

$$r^* = \begin{cases} 0 & N_F = 2 \\ \simeq 0.6 & N_F = 3 \\ 1 & N_F > 3 \end{cases} \quad (5)$$

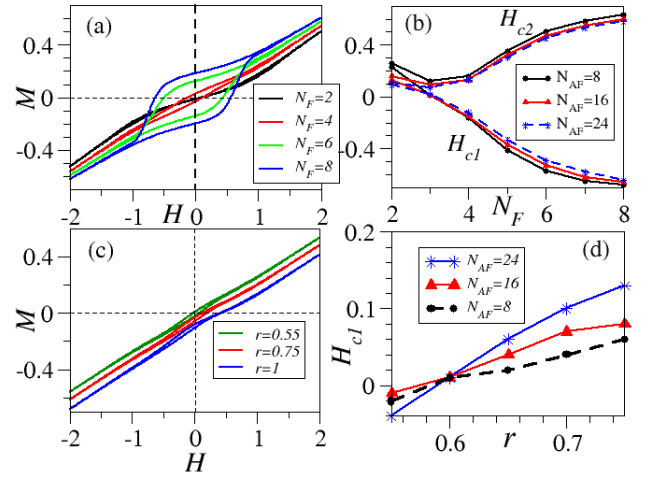


FIG. 8: (Color online) (a) Hysteresis loop of two-dimensional heterostructures of  $N_F$  ferromagnetic layers on the top of  $N_{AF} = 24$  antiferromagnetic layers. Here the length of each layer is  $L = 128$ ,  $\uparrow$ -spin fraction  $r = 0.6$ . (b) The dashed line shows  $H_{c1}$  and  $H_{c2}$  as a function of  $N_F$ . Similar curves for  $N_{AF} = 16, 8$  are also shown here (solid lines). (c) Hysteresis curves for different  $r$ , for a heterostructure with  $N_{AF} = 8$  and  $N_F = 3$ . Corresponding values of  $H_{c1}$ , as a function of  $r$ , is shown (dashed-line) in (d). In panel (d) we have also plotted similar curves for different  $N_{AF} = 16, 24$ . This indicates that for a heterostructure with three ferromagnetic layers ( $N_F = 3$ ),  $H_{c1}$  becomes positive when  $\sim 60\%$  of the pinned spins are  $\uparrow$ . The unspecified parameters here are same as in Eq. (3).

For  $N_F = 2$   $H_{c1}, H_{c2}$  are positive for any  $r > 0$ , whereas for  $N_F > 3$ , coercive field  $H_{c1}$  is negative for any  $r > 0$ .

## V. WHY PINNING AFFECTS HYSTERESIS ?

What we observe so far from the Monte Carlo simulation of the core-shell nanostructure is that, irrespective

of shape, size, value of the interaction strength and pinning parameters, the exchange bias  $H_{eb}$  increases with increase of pinning density  $\eta$  and decrease with  $\uparrow$  spins fraction  $r$ . To understand this, we introduce a simple model of the surface ignoring the interaction of the surface spins with those in the bulk (shell). In two dimensional core-shell structure of Ising spins, the surface is as a one dimensional chain with periodic boundary condition; the corresponding Hamiltonian is now,

$$\mathcal{H}_{surf} = -J_{sh} \sum_{i=1}^L s_i s_{i+1}, \quad (6)$$

where  $L$  is total number of spins on the surface. For a circular core-shell structure studied here,  $L \simeq 2\pi R$ ; in fact a better approximation is  $L \simeq 4R$ , since for every  $i \in (-R, R)$  there are two boundary spins. We assume that  $N$  spins on the surface are pinned, of which  $N_+$  spins are  $\uparrow$ , thus  $\sum_k S_k = 2N_+ - N = M_b$ . Accordingly,

$$\eta = \frac{N}{L}, \quad r = \frac{N_+}{N} \quad \text{and} \quad m_b \equiv \frac{M_b}{N} = 2r - 1. \quad (7)$$

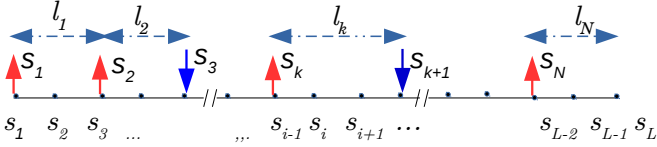


FIG. 9: (Color online) The pinned spins are denoted  $\{S_1, S_2, \dots, S_N\}$ . Here  $S_1 = s_1, S_2 = s_3, \dots, S_N = s_{L-2}$ . Distance between two consecutive pinned spins  $S_k$  and  $S_{k+1}$  is  $l_k$ . The periodic boundary condition ensures that  $s_{i+L} = s_i$  and  $S_{k+N} = S_k$ .

For notational convenience, let us denote the pinned spins as  $\{S_1, S_2, \dots, S_N\}$  with  $S_1 = s_{i_{min}}$ , where  $i_{min}$  is the position index of the first pinned spin (see Fig. 9). As shown in the figure, the separation of two consecutive pinned spins  $S_k$  and  $S_{k+1}$  is  $l_k$ .

The partition function of the system can be written as

$$\begin{aligned} Z_{L,N}(\{l_i\}) &= \sum_{\{s_i\}} e^{-\beta \mathcal{H}_{surf}} \\ &= \prod_{k=1}^N \langle S_k | T^{l_k} | S_k \rangle \delta \left( \sum_{k=1}^N S_k - M_b \right), \quad (8) \end{aligned}$$

where  $T = \begin{pmatrix} e^K & e^{-K} \\ e^{-K} & e^K \end{pmatrix}$  with  $K = \beta J_{sh}$  is the usual transfer matrix of one-dimensional Ising model, and  $K = \beta J_{sh}$ .

In presence of the constraint, that exactly  $N_+$  out of  $N$  pinned spins are  $\uparrow$ , which is ensured by a  $\delta$ -function

in above equation, evaluating this partition-sum (8) is difficult. We proceed to find a generating function of  $Z_{L,N}(\{l_i\})$ ,

$$\begin{aligned} \mathcal{Z}_L(x) &= \sum_{M_b=0}^{\infty} Z_{L,N}(\{l_i\}) x^{M_b} = \text{Tr} \left[ \prod_{k=1}^N (T^{l_k} A) \right], \quad (9) \\ \text{where } A &= \sum_{S_k=\pm} x^{S_k} |S_k\rangle \langle S_k| = \begin{pmatrix} x & 0 \\ 0 & x^{-1} \end{pmatrix} \quad (10) \end{aligned}$$

Eigenvectors of  $T$  are  $|\pm\rangle = \begin{pmatrix} 1 \\ \pm 1 \end{pmatrix}$  with eigenvalues  $\lambda_{\pm} = e^K \pm e^{-K}$ , the generating function  $\mathcal{Z}_L(x)$  can be evaluated using the diagonalizing matrix  $U = \frac{1}{\sqrt{2}} \begin{pmatrix} 1 & 1 \\ 1 & -1 \end{pmatrix}$ .

$$\mathcal{Z}_L(x) = \lambda_+^L \left( x + \frac{1}{x} \right)^N \left[ 1 + \left( \frac{\lambda_-}{\lambda_+} \right)^{l^*} \left( \frac{x^2 - 1}{x^2 + 1} \right)^2 + \dots \right] \quad (11)$$

where, we have used  $\sum_{k=1}^N l_k = L$  and  $l^* = \text{Min}(\{l_i\})$  is the smallest separation between consecutive pinned spins.

Note that, for any given choice of separations  $\{l_k\}$ , one can calculate  $\mathcal{Z}_L(x)$  explicitly using Eq. (11). In the second step here, we use a perturbation series in  $\lambda = \frac{\lambda_-}{\lambda_+} = \tanh(\beta J_{sh})$ , valid quite well in large temperature limit. The dominant (zeroth order) term of  $\mathcal{Z}_L(x)$  does not depend on individual separations  $\{l_k\}$ , and the next order correction depends only on the smallest separation  $l^*$ . We have assumed that the smallest separation  $l^*$  appear only once in  $\{l_k\}$ ; if it appears  $n$  times (and the separations are not adjacent to each other) then we have an additional multiplicative factor  $n$ ,

$$\mathcal{Z}_L(x) \simeq \lambda_+^L (x + x^{-1})^N \left[ 1 + n \lambda^{l^*} \left( \frac{x^2 - 1}{x^2 + 1} \right)^2 \right] \quad (12)$$

The average value of  $M_b$  is now

$$\begin{aligned} \langle M_b \rangle &= x \frac{d}{dx} \ln \mathcal{Z}_L(x) \\ &= N \frac{x^2 - 1}{x^2 + 1} + \frac{4n \lambda^{l^*} x^2}{(1 + x^2)^2 + n \lambda^{l^*} (x^4 - 1)} \quad (13) \end{aligned}$$

Further, by redefining  $x = e^{-\beta h}$ , one can check from Eq. (9) that  $\mathcal{Z}_L(x)$  is the partition function of an effective Hamiltonian

$$\tilde{\mathcal{H}}_{surf} = -J_{sh} \sum_{i=1}^L s_i s_{i+1} - h \sum_{k=1}^N S_k, \quad (14)$$

where the magnetic field  $h$  is acting *selectively* only on the pinned spins. Thus the thermodynamic description of a system having  $M_b$  number of excess  $\uparrow$ -spins among  $N$  pinned ones, is equivalent to a system without pinning, but an additional magnetic field  $h$  acting only on the

pinned spins. The value of  $h$ , for any given  $r$ , can be calculated from Eqs. (13) and (7) as

$$r = \frac{1}{2} \left( 1 + \tanh(\beta h) + \frac{1}{N} \frac{n\lambda l^* \operatorname{sech}(\beta h)^2}{1 - n\lambda l^* \tanh(\beta h)} \right). \quad (15)$$

This additional field on the pinned spins, along with an external magnetic field  $H$ , produce an effective field per site,

$$H_{eff} = H + \eta h \quad (16)$$

In this system, the hysteresis loop would be symmetric if the curves are plotted against  $H_{eff}$ . But, if it is plotted against the external field  $H$ , the curves would become asymmetric, in fact shifted by  $\eta h$ . Then, the exchange bias is expected to be

$$H_{eb} = \eta h \quad (17)$$

In the large  $N$  limit, it is reasonable assume that the smallest separation between two consecutive spins is  $l^* = 1$ ; in this limit Eq. (15) to a leading order in  $N$  we have,

$$h = \frac{1}{\beta} \tanh^{-1}(m_b) + \frac{1}{\beta N} \frac{n\lambda}{n\lambda m_b - 1}. \quad (18)$$

The effective field  $h$ , along with Eq. (17), indicates that the exchange bias increases linearly, with pinning density  $\eta$  and temperature  $\beta^{-1}$ ; it also grows monotonically with  $m_b$  or  $r = \frac{1+m_b}{2}$ . Linear dependence of  $H_{eb}$  on  $\eta, r$  are observed in Fig. 2 (a) and (b) respectively. We have also observed linear temperature dependence of  $H_{eb}$  from Monte Carlo simulations of inverse core-shell nanoparticles (figures are not presented here).

Note that the interaction strength  $J_{sh}$ , appears in Eq. (18) in the second term through the relation  $\lambda = \tanh(\beta J_{sh})$ , is suppressed by the factor  $N$ . Thus, the dependence of  $H_{eb}$  on the interaction strength  $J_{sh}$  is negligible. This is indeed observed from simulations results described in Fig. 2 (c).

It is interesting that a simple model of the surface that clearly ignore the interaction of the surface spins with other spins in the shell reproduce the properties of hysteresis qualitatively.

## VI. CORE-SHELL STRUCTURES IN THREE DIMENSION

In three spatial dimensions, magnetic phase transition can occur in systems having discrete (Ising) or continuous spins (like XY and Heisenberg). In this section we extend our study to core-shell structures with spin interactions given by either Ising, XY or Heisenberg models. We study the hysteresis properties of three models, separately, on a cubical core-shell with core  $\mathcal{C}$  of length  $R_c$

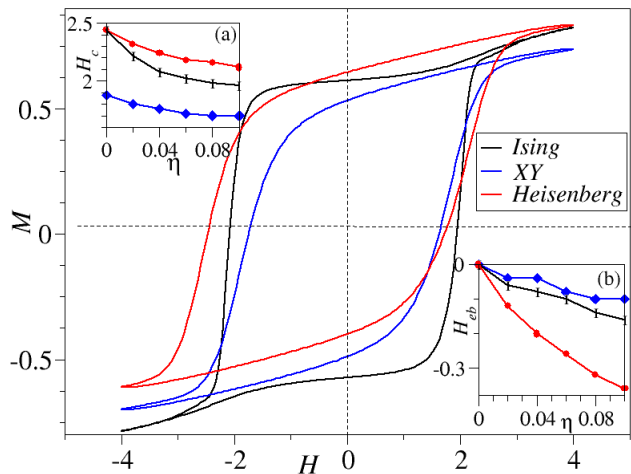


FIG. 10: (Color online) Hysteresis loops of a cubical core-shell structure (particle size  $R^3$  and core size  $R_c^3$ ) for Ising, XY and Heisenberg models, with  $R_c = 26$ ,  $R = 32$ , pinning density  $\eta = 0.1$  and interaction parameters  $J_c = -0.5$ ,  $J_{sh} = 1$ ,  $J_{int} = 1$ . The insets (a) and (b) respectively shows variation of  $H_c$  and  $H_{eb}$  as a function of  $\eta$ . Heisenberg models generate maximum exchange bias  $|H_{eb}|$  and coercivity  $H_c$ .

and shell  $\mathcal{S}$  of width  $R - R_c$ , i.e., we have a cubical core of size  $R_c^3$  and particle size  $R^3$ .

The Hamiltonian of the system is now,

$$\mathcal{H} = -J_c \sum_{i \in \mathcal{C}, j \in \mathcal{C}} \mathbf{S}_i \cdot \mathbf{S}_j - J_{sh} \sum_{i \in \mathcal{S}, j \in \mathcal{S}} \mathbf{S}_i \cdot \mathbf{S}_j - J_{int} \sum_{i \in \mathcal{S}, j \in \mathcal{C}} \mathbf{S}_i \cdot \mathbf{S}_j - H \sum_{i \in \mathcal{C}, i \in \mathcal{S}} S_i^x, \quad (19)$$

Now spins  $\mathbf{S}_i$  at lattice site  $i$  is a unit vector, i.e.,  $\mathbf{S}_i \cdot \mathbf{S}_i = 1$ , and ‘ $\cdot$ ’ corresponds the usual dot-product of vectors. For Heisenberg model  $\mathbf{S}_i = (S_i^x, S_i^y, S_i^z)$  has three components, for XY-model  $\mathbf{S}_i = (S_i^x, S_i^y)$  has two components. For the Ising spins  $\mathbf{S}_i \equiv S_i^x = \pm 1$  and dot-product in Eq. (19) is interpreted as simple multiplication. The direction of the magnetic field is taken as the  $x$ -axis.

We also consider that some of the spins on the surface are pinned, and their density is  $\eta$ . In other words,  $\eta$  fraction of total number of spins on the surface, having  $6R^2 - 12R + 8$  sites in total, are pinned. We also assume that all the pinned spins are aligned along a particular direction, chosen to be  $x$ -direction. Note that for core-shell structure in two dimension, surface pinning is characterized by two parameters, the pinning density  $\eta$  and  $\uparrow$ -spin fraction  $r$ . That all the pinned spins here are parallel to each other is equivalent to  $r \equiv 1$ , where pinning effects are maximum.

Now we compare the hysteresis curves obtained from Monte Carlo simulations of all the three models on a core-shell structure with  $R_c = 26$  and  $R = 32$ , which means that the width of the shell is 6 lattice units. The

interaction parameters are taken as  $J_c = -0.5$ ,  $J_{sh} = 1$ ,  $J_{int} = 1$ . In Fig. 10 we have plotted the hysteresis curves for  $\eta = 0.4$ . The insets (a) and (b) in Fig. 10 shows respectively the variation of  $H_c$  and  $H_{eb}$  as a function of pinning density  $\eta$ . In all three model, the coercivity  $H_c$  goes down with increase of  $\eta$ , whereas as expected,  $|H_{eb}|$  increases. For Heisenberg model, both the coercivity and the change in exchange bias is quite high compared to that of other models.

Asymmetric hysteresis, and thus large exchange bias, has been observed earlier in core-shell nanostructures. For ferromagnetic core and antiferromagnetic shell, one of the primarily factor that controls the magnetic properties is the core-shell interaction parameter. Numerical studies of these core-shell structures with Heisenberg spin interactions, additional anisotropic spin interaction and crystal field claims that, under field cooled conditions, the exchange bias strongly depends on the nature and strength of core-shell interaction [36, 47]. Here we show that surface pinning can affect the exchange bias strongly, even in the zero field cooled conditions and in absence of anisotropy or crystal fields. This pinning effect is quite dominant in inverse core-shell nanostructures where the core is antiferromagnetic and the shell, ferromagnetic.

## VII. DISCUSSIONS AND CONCLUSION

Wide variation in magnetic properties has been observed in nano-materials. In this mesoscopic scale, the size, shape and intrinsic spin interactions play a significant role. This leads to many fascinating finite size effects [59] like, magnetic anisotropy [60], unusual magnetization [61] and superparamagnetic behavior [62]. In addition, external perturbations on nanoparticles, like temperature, pressure and different solvent conditions can tune the magnetic properties in interesting ways; organic solvents are known agents which may pin the spins on the surface [41].

In this article we study how magnetic properties are modulated in core-shell nanostructures and heterostructures when some of the spins on the surface get pinned. We find that, for core-shell nanoparticles, the hysteresis behavior is significantly modified when the shell is ferromagnetic and the core is antiferromagnetic, i.e., in a inverse core-shell structure. Ferromagnetic cores or antiferromagnetic shells are not affected much by surface pinning. Thus, we primarily focus on the inverse core-shell structure and study hysteresis in zero field cooled conditions using Monte Carlo simulations. We find that the exchange bias  $H_{eb}$  changes linearly with pinning density  $\eta$  and its sign changes from being positive to negative when the  $\uparrow$ -pinning fraction  $r$  is increased beyond  $r = \frac{1}{2}$ . The dependence of  $H_{eb}$  on  $J_{int}$  is found to be negligible.

To understand these variations we also propose a simple model of the surface in V. For the two dimensional

inverse core shell structure, the surface is an one dimensional ring, where Ising spins interact with coupling strength  $J_{sh}$ . We show that the pinning of spins can generate an effective magnetic field in the positive (negative) direction when the fraction of  $\uparrow$ -spins  $r$  is greater (smaller) than  $\frac{1}{2}$ ; accordingly, a negative (positive) exchange bias  $H_{eb}$  is generated in the inverse core-shell structure. We show explicitly, in Eq. (17), that the magnitude  $H_{eb}$  is proportional to  $\eta$ . The effective field is found to be independent of number of pinned spins  $N$  in leading order and it varies as  $\frac{1}{N}$  as a next order correction. Interaction strength  $J_{sh}$  appears only in the correction term which is negligible for large  $N$ . This simple model of surface, though ignores the interaction of spins on the surface with other spins in the shell, explains the qualitative properties of the hysteresis quite well.

The following comment is in order. In absence of pinning, core-shell structures in three dimension, under field cooled conditions, exhibit strong dependence of exchange bias on interface interaction  $J_{int}$  [36, 47] due to uncompensated spins at the interface. Most models that study these behavior considered the presence of spin anisotropic interactions and crystal field in the system. In absence of these complexities, in the present study of inverse core-shell structure we find a large exchange bias, even in zero field cooled condition when surface spins are pinned. The dependence of  $H_{eb}$  on  $J_{int}$ , however, turns out to be very weak.

To understand how shell thickness affect the exchange bias and coercivity, we increase the core size  $R_c$  for a given  $R$ . This resulted in lower coercivity, but  $|H_{eb}|$  is not affected much since the surface area (where spin-pinning occurs) does not change. Increase of  $R$  and  $R_c$  proportionately, with a fixed  $R_c/R$ , generates a thermodynamically large core-shell structure. In this case too the coercivity increases because the ferromagnetic shell is larger in size, but the exchange bias decreases as because the surface to volume ratio decreases. Clearly, the asymmetry in the hysteresis disappears in the thermodynamic limit indicating that the emergence of exchange bias is only a mesoscopic phenomena.

In addition, we also study the core-structures of different shapes, namely triangular, square, circular, elliptical and some irregular shapes. Both, the value of coercive field  $H_c$  and exchange bias  $|H_{eb}|$  changes non-trivially. We separately investigate the role of aspect ratio of an elliptical core-shell structure and find that the coercivity  $H_c$  decreases, but  $|H_{eb}|$  increases with aspect ratio, re-confirming the fact a rod-like nanostructure may have the smallest coercivity [58].

We also investigate the nanoscale heterostructures of ferromagnetic layers grown on the top of antiferromagnetic layers, by introducing spin pinning in the top and bottom surfaces. Like in core-shell structures, here too the exchange bias is proportional to the pinning density and it changes sign when  $\uparrow$ -spin fraction  $r$  is increased

beyond  $\frac{1}{2}$ . The coercivity, as expected, depends strongly on the number of ferromagnetic layers. An interesting finite size effect is observed: it turns out that there are three or less ferromagnetic layers, the coercive field  $H_{c1}$  changes from being negative to positive when  $\uparrow$ -spin fraction crosses a threshold value  $r^*$ ;  $r^*$  does not depend on the number of antiferromagnetic layers.

In conclusion, we study in detail the effect of surface pinning on magnetic properties of two dimensional core-shell nanostructures and heterostructures in nanoscale, where spin interactions are considered Ising-like. The pinning effect turns out to be more prominent in a inverse core-shell structure where spin interact antiferromagnetically in the core and ferromagnetically in the shell. Studying variation of hysteresis by changing interaction and pinning parameters in Monte Carlo simulations we conclude that the exchange bias increases with increase of pinning density and the fraction of  $\uparrow$ -spins which are pinned. This behavior could be explained from the analytical studies of a model introduced here that captures only the interaction of pinned spins on the surface. The shape and size of the nanoparticles, which can be tuned experimentally, also strongly modify the exchange bias and coercivity. The results obtained in two dimension, with Ising spins, are found to be robust in three dimension irrespective of whether the spins interact following Ising, XY- or Heisenberg models. We believe that the new mechanism of exchange bias generated from the pinning of spins on the surface, whose morphology and pinning density can be changed easily, will help in providing fruitful technological applications in future.

AS acknowledges support from DST-INSPIRE in the form a Senior Research Fellowship. PKM acknowledges support from the Science and Engineering Research Board (SERB), India, Grant No. TAR/2018/000023.

---

[1] *Introduction to Nanotechnology*, Jr. Poole and P. Charles, John Willy & Sons, Inc., New Jersey (2003).  
 [2] *Nanostructures and Nanomaterials*, G. Cao and Y. Wang, World Scientific, London (2011).  
 [3] P. Claus, A. Brückner, C. Mohr, and H. Hofmeister, *J. Am. Chem. Soc.* **122**, 11430 (2000).  
 [4] *Molecular Nanomagnets*, D. Gatteschi, R. Sessoli, and J. Villain, Oxford University Press, UK (2011).  
 [5] I. Khan, K. Saeed, I. Khan, *Arab. J. Chem.* (2017)(in press)  
 [6] T. K. Indira, P. K. Lakshmi, *Int. J. Pharm. Sci. Nanotech.* **3**, 1035 (2010).  
 [7] M. Gibertini, M. Koperski, A. F. Morpurgo and K. S. Novoselov, *Nat. Nanotech.* **14**, 408 (2019).  
 [8] M-Y. Li, C-H. Chen, Y. Shi, and L-J. Li, *Materials Today* **19**, 322 (2016).  
 [9] S. Bhattacharya and S. K. Saha, *Macromol. Symp.* **376**, 1600183 (2017).

[10] B. Heblar *et. al.*, *Phys Rev. B* **95**, 104410 (2017).  
 [11] T. Song *et. al.*, *Science* **360**, 1214 (2018).  
 [12] K. Tivakornsasithorn *et. al.*, *Sci. Rep.* **8**, 10570 (2018).  
 [13] J. H. Garcia *et. al.*, *Chem. Soc. Rev.* **47**, 3359 (2018).  
 [14] F. Huang, X. Xu, X. Lu, M. Zhou, H. Sang, and J. Zhu, *Sci. Rep.* **8**, 2311 (2018).  
 [15] R. Liu and R. D. Priestley, *J. Mat. Chem. A* **4**, 6680 (2016).  
 [16] R. G. Chaudhuri, S. Paria, *Chem. Rev.* **112**, 2373 (2012).  
 [17] S. Laurent *et. al.* *Chem. Rev.* **108**, 2064 (2014).  
 [18] I. K. Herrmann *et. al.*, *Small* **6**, 1388 (2010).  
 [19] Q. Zhang *et. al.*, *Acc. Chem. Res.* **46**, 1816 (2013).  
 [20] C. T. Lo *et. al.*, *Chem. Commun.* **52**, 7269 (2016).  
 [21] D. Sudfeld *et. al.*, *IEEE Trans. Magn.* **38**, 2601 (2002).  
 [22] M. J. Kinsella *et. al.*, *J. Phys. Chem. C* **112**, 3191 (2008).  
 [23] C. Goubault *et. al.*, *J. Phys. Rev. Lett.* **91**, 260802 (2003).  
 [24] M. Tabuchi *et. al.*, *Nat. Biotech.* **22**, 337 (2004).  
 [25] J. Jia *et. al.*, *ACS Appl. Mater. Interfaces.* **9**, 2579 (2010).  
 [26] H. Wang *et. al.*, *ACS Appl. Mater. Interfaces* **6**, 15309 (2014).  
 [27] J. McCathy *et. al.*, *Adv. Drug Deliv. Rev.* **60**, 1241 (2008).  
 [28] S. Xuan, Y. X. J. Wang, J. C. Yu, and K. C. F. Leung, *Langmuir* **25**, 11835 (2009).  
 [29] Z. D. Vatansever, *Phys. Lett. A* **382**, 2901 (2018).  
 [30] E. A. Kwizera *et. al.*, *Phys. Chem. C* **120**, 10530 (2016).  
 [31] Q. Rong, A. Zhu, and T. Zhong, *J. Appl. Polym.* **120**, 3654 (2011).  
 [32] J. F. Li *et. al.*, *Langmuir*, **22**, 10372 (2006).  
 [33] S. E. Shirsath *et. al.*, *Sci. Rep.* **6**, 30074 (2016).  
 [34] M. Vasilakaki, K. N. Trohidou, and J. Nogués, *Sci. Rep.* **5**, 9609 (2015).  
 [35] S. Chandra, H. Khurshid, M-H. Phan, and H. Srikanth, *Appl. Phys. Lett.* **101**, 232405 (2012).  
 [36] O. Iglesias, X. Batlle, and A. Labarta, *Phys. Rev. B*, **72**, 212401 (2005).  
 [37] Q. K. Ong and A. Wei, *Phys. Rev. B* **80**, 134418 (2009).  
 [38] E. C. Sousa *et. al.*, *J. Appl. Phys.* **106**, 093901 (2009).  
 [39] *Statistical Mechanics: Rigorous Results*, D. Ruelle, (Addison-Wesley, Reading, 1989).  
 [40] N. D. Mermin and H. Wagner, *Phys. Rev. Lett.*, **17** 1133 (1966).  
 [41] A. E. Berkowitz, J. A. Lahut, I. S. Jacobs, and L. M. Levinson, *Phys Rev. Lett.* **34**, 594 (1975).  
 [42] M. Sparks, *Phys Rev. Lett.* **22**, 1111 (1969).  
 [43] M. Vasilakakz, K. N. Trohidou, and J. Nogués, *Sci. Rep.*, **5**, 1 (2015).  
 [44] To obtain hysteresis, the temperature must be lower than the critical value; here  $\beta^{-1} = 1$  is much smaller than the critical temperature  $T_c = \frac{2}{\ln(1+\sqrt{2})}$  of Ising model on a square lattice with interaction strength  $J = 1$ .  
 [45] R. Wu *et. al.*, *Phys. Rev. B* **97**, 024428 (2018).  
 [46] E. Eftaxias and K. N. Trohidou, *Phys. Rev. B* **71**, 134406 (2005).  
 [47] J. Nogués, D. Lederman, T. J. Moran, and I. K. Schuller, *Phys. Rev. Lett.* **76** 4624 (1996).  
 [48] A. Zaim and M. Kerouad, *Physica A*, **389** 3435 (2010).  
 [49] X. Sun *et. al.*, *Nano Lett.* **12**, 246 (2012).  
 [50] B. Khodashenas, H. R. Ghorbani, *Arab. J. Chem.* **2015** (in press); *J. Helmlinger et. al.*, *RSC Adv.* **6**, 18490 (2016).  
 [51] Y. Zhao *et. al.*, *Sc. Rep.* **7**, 4131 (2017).

- [52] A. J. Champion, Y. K. Katare, and S. Mitragotri, PNAS **104**, 11901 (2007); W Zhang, R. Singh, N. Bray-Ali, and S. Haas, Phys. Rev. B. **77**, 144428 (2008).
- [53] H. Jia *et. al.*, Spectrochim. Acta. A. Mol. Biomol. Spectrosc. **64** 956(2006).
- [54] C. A. Little, C. Batchelor-McAuley, N. P. Young, and R. G. Compton, Nanoscale **10**, 15943 (2018).
- [55] Q. Song and Z. John Zhang, J. Am. Chem. Soc. **126** 6164(2004).
- [56] J. Zwara *et. al.*, Journal of J. Photochem. Photobiol. A **367** 240(2018).
- [57] J. Hu *et. al.*, RSC Adv. **8**, 21505(2018).
- [58] A. Sahoo and D. Bhattacharya, Journal of Alloy and Compounds, **772**, 193(2019).
- [59] G. C. Papaefthymiou, Nano Today **4**, 438 (2009).
- [60] M. Jamet *et. al.*, Phys. Rev. Lett. **86**, 4676 (2001).
- [61] S. E. Apsel, J. W. Emmert, J. Deng, and L. A. Bloomfield, Phys. Rev. Lett. **76**, 1441 (1996).
- [62] Wahajuddin and S. Arora, Int. J. Nano Med. **7**, 3445 (2012).